Electronic Supplementary Material (ESI) for Nanoscale Advances.

Supplementary Information

3D Fluorescence Confocal Microscopy of InGaN/GaN Multiple Quantum Well Nanorods from light absorption perspective

Yan Gu[a,b], Yu shen Liu[c], Guofeng Yang[b],*, Feng Xie[d], Chun Zhu[b], Yingzhou Yu[b], Xiumei Zhang[b], Naiyan Lu[b], Yueke Wang[b] and Guoqing Chen[b]

[a] School of Internet of Things, Jiangnan University, Wuxi 214122, China

[b] School of Science, Jiangsu Provincial Research Center of Light Industrial Optoelectronic Engineering and Technology, Jiangnan University, Wuxi 214122, China

[c] School of Electronic and Information Engineering, Changshu Institute of Technology, Changshu 215556, China

[d] The 38th Research Institute of China Electronics Technology Group Corporation, Hefei 230000, China

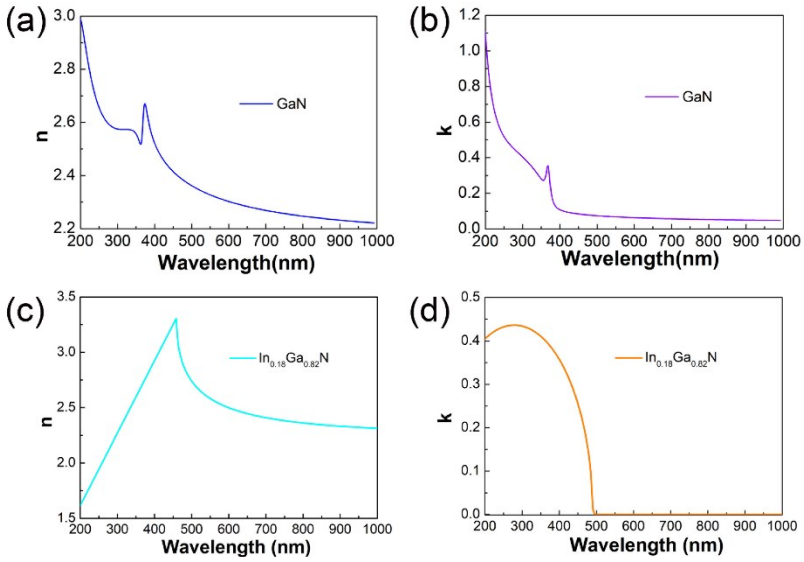

Fig. S1. (a) Real (n) and (b) imaginary (k) values of the refractive index for GaN in simulations. (c) Real (n) and (d) imaginary (k) values of the refractive index for $In_{0.18}Ga_{0.82}N$ in simulations.

Optical parameters (complex-valued refractive index) for GaN material obtained from the study of Kawashima et al [1] are plotted in Fig. S1(a). The Adachi model [2, 3] is employed to calculate the wavelength-dependent real part of refractive index parameter n for $In_xGa_{1-x}N$. Adachi model is expressed as [2]

$$n = sqrt\left\{ A\left(\frac{E}{E_g}\right)^{-2}\left[2-\sqrt{1+\left(\frac{E}{E_g}\right)}-\sqrt{1-\left(\frac{E}{E_g}\right)}\right]+B\right\},$$

where E is photon energy, E_g is bandgap energy of $In_xGa_{1-x}N$ [4], A and B are fitting constants which are given by [3]

$$A = 53.57x + 9.84(1-x)$$
$$B = -9.19x + 2.74(1-x)$$

according to different In-content.

The extinction coefficient as the imaginary part of the complex refractive index is defined as

$k = \frac{\partial(E)g\lambda}{4\pi}$, where λ is wavelength and *α(E)* is the absorption coefficient as a function of photon energy. *α(E)* can be expressed as [5]

$\partial(E) = 10^5\sqrt{a\cdot(E-E_g)+(E-E_g)^2}\,cm^{-1}$, where the values of a, b can be obtained by linear interpolation [5], as following

$$a = -2.85511x + 2.80786$$
$$b = 1.24246x - 0.36815$$

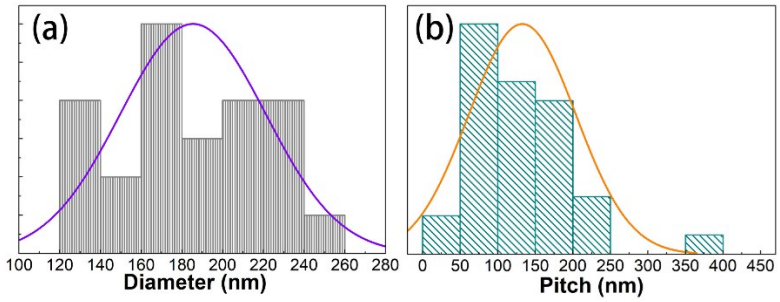

Fig. S2. (a) Diameter and (b) distributions for the InGaN/GaN MQW NRs displayed in fig. 3(b).

Fig. S2(a) and (b) display the diameter and pitch distributions of the array have been discussed, for which standard deviations of σ = 35.3 nm and 71 nm are extracted, respectively. The diameters of which are all >100nm, which fit the "nanorod" criteria. According to the report [6], it can be concluded that no obvious absorption peaks are formed in the case of random and non-periodic nano-structure, owing to the failure to provide one major mode which the incident light can couple into the NWs for randomly spaced NRs. In addition, this will also contribute to the observation of lower absorption compared to the highly ordered array.

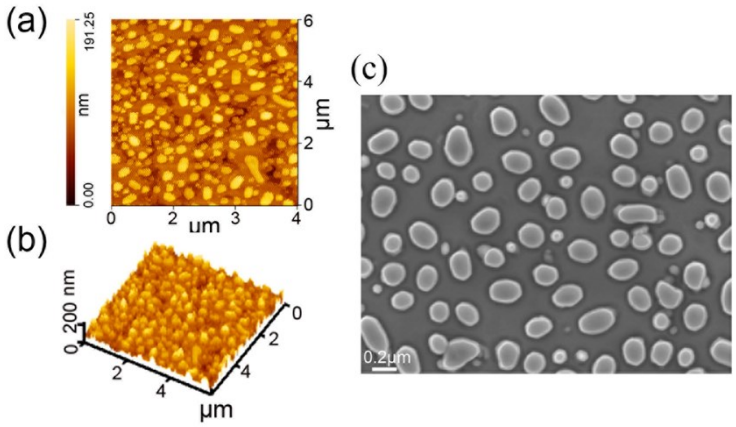

Fig. S3. (a) AFM 2D image, (b) 3D image and (c) Top-view SEM image of Ni self-organized nanoparticles on InGaN/GaN MQWs surface after RTA for 3min at 800℃, respectively.

Fig. S3 demonstrates the characteristics and morphology of Ni nanoparticles after RTA process. It can be seen from the AFM images of Ni nanoparticles shown in Fig. S3(a) and (b) that a clear nano-islands structure is formed after RTA for 3min at 800 ℃, which can meet the requirements of etching mask. Fig. S3(c) presents the top-view SEM image of Ni nano-islands fabricated with Ni film annealed at temperature of 800 ℃ for 3 mins by RTA process. It can be clearly seen that the diameter of self-assembly nanoparticle masks distributed on the surface of the quantum well is about 250nm. Therefore, the production of nano-scale masks for nanorods can be achieved through a simple process.

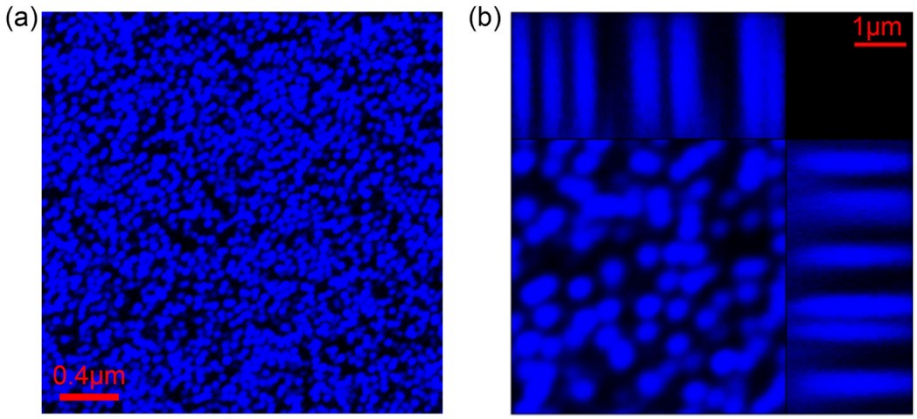

Fig. S4. (a) 2D confocal picture of nanorod taken at low magnification. (b) 3D image was created by combining z stack with an internal xy-plane distance of 93nm.

A confocal picture of nanorods emitting blue fluorescence under low magnification is presented in Fig. S4(a). On this basis, 3D confocal image of nanorods composed of z-stacks of 2D images with a vertical distance of 93 nm between each image is observed under high magnification.

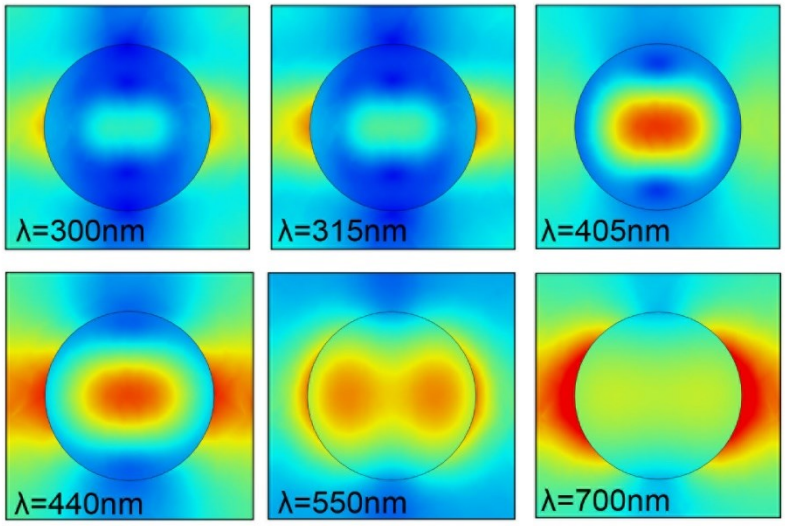

Fig. S5. The top view electric fields at z=120nm for both resonant and non-resonant wavelengths.

Fig. S5 depicts the xy-plane cross-section electric field diagrams at z=120nm. It can be seen that the electric field inside the nanorod at the resonance wavelength is stronger than that at the non-resonant wavelength.

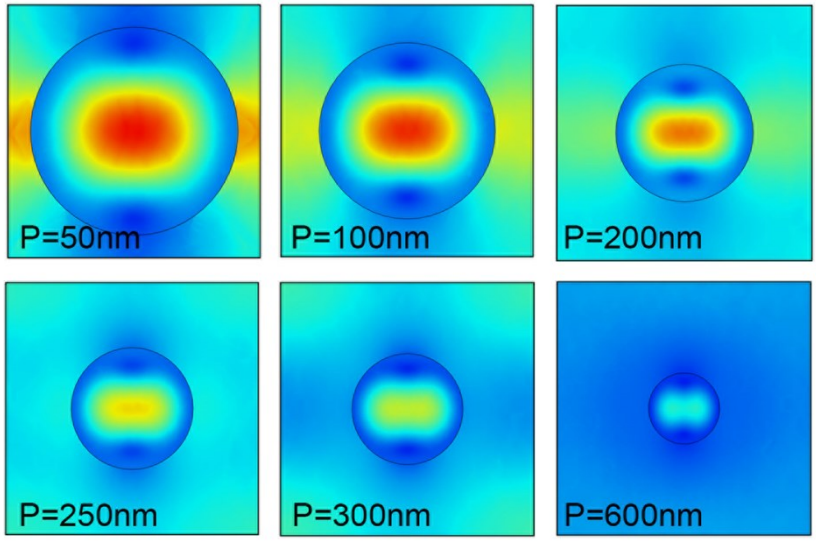

Fig. S6. The radial (x-y) cross-sections electric field diagrams of nanorod arrays for P=50nm, 100nm, 200nm, 250nm, 300nm and 600nm at z=120nm.

Fig. S6 plots the top view electric fields at z=120nm for wavelength of 405nm. Obviously, the electric field becomes weaker as the distance between the neighboring nanorods increases, so the absorption decreases.

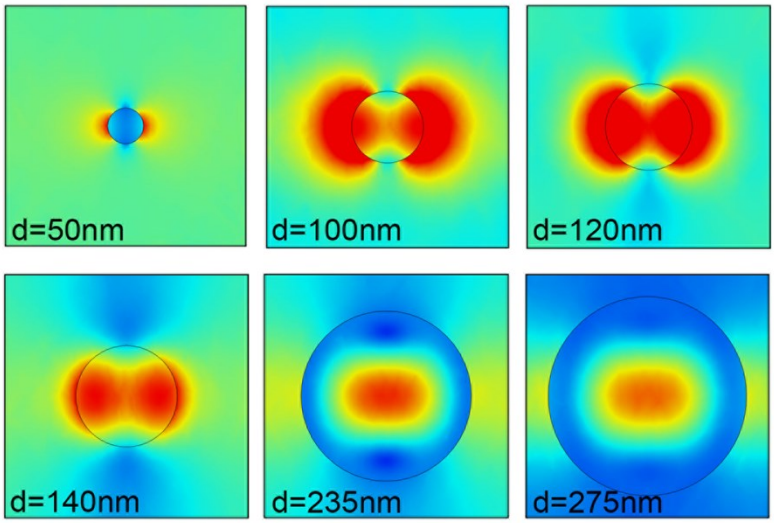

Fig. S7. The xy-plane (z=120nm) electric filed distributions of nanorods for d=50nm, 100nm, 120nm, 140nm, 235nm, and 275nm at λ=405nm.

It is clear from the xy-plan electric filed distributions shown in Fig. S6 that most of the electric field is in the nanorod for diameters ≥120nm. While the electric field for a diameter of 50 nm is almost distributed in the air, and there is no electric field in the nanorod. As a result, the absorption of the nanorods with D=120nm due to the strongest electric field of nanorods for diameter of 120nm.

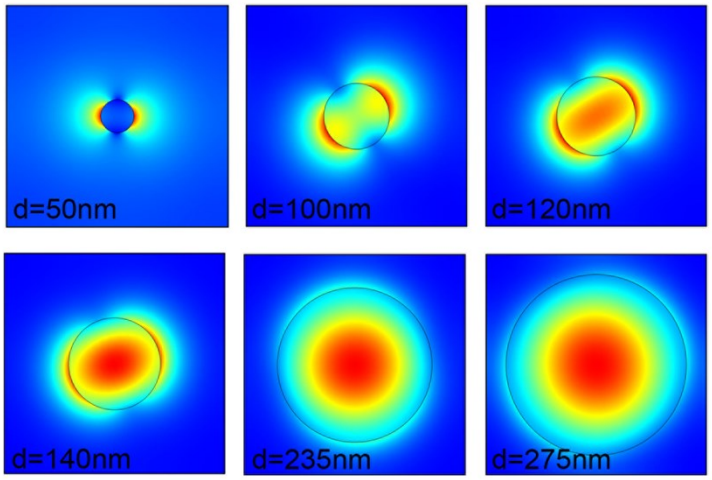

Fig. S8. The modal fields of the fundamental mode under different diameters for resonance wavelength.

Fig. S8 shows the fundamental mode field diagrams of nanorods with different diameters. It can be obtained that the effective refractive index of 1.015 for a diameter of 50 nm is close to that of air by modal analysis. Furthermore, the confinement of the electric field within the nanorod is enhanced as the diameter of the nanowire becomes larger.

References

1. T. Kawashima, H. Yoshikawa, S. Adachi, S. Fuke, K. Ohtsuka, *J. Appl. Phys.*, 1997, **82**, 3528-3535.
2. S. Adachi, *J. Appl. Phys.*, 1982, **53**, 5863-5869.
3. J. Piprek, *UCSB: Academic.*, 2003, **93**.
4. J. Wu, W. Walukiewicz, K. M. Yu, J. W. Ager, E. E. Haller, H. Lu, W. J. Schaff, Y. Saito, Y. Nanishi, *Appl. Phys. Lett.*, 2002, **80**, 3967-3969.
5. G. F. Brown, J. W. Ager, W. Walukiewicz, J. Wu, *Sol. Energy Mater. Sol. Cells*, 2010, **94**, 478-483.
6. J. Treu, X. Xu, K. Ott, K. Sailer, G. Abstreiter, J. J. Finley, G. Koblmuller, *Nanotechnology*, 2019, **30**, 8.